Available online at www.sciencedirect.com

ScienceDirect

Energy Procedia 95 (2016) 167 – 174

Energy Procedia

International Scientific Conference "Environmental and Climate Technologies", CONECT 2015, 14-16 October 2015, Riga, Latvia

Validation of unglazed transpired solar collector assisted air source heat pump simulation model

Karolis Januševičius*, Giedrė Streckienė, Juozas Bielskus, Vytautas Martinaitis

Vilnius Gediminas Technical University, Sauletekio ave. 11, Vilnius, LT–10223, Lithuania

Abstract

Due to the rising demand for high comfort standards and efficient energy use, heat pumps and solar technologies have drawn a great deal of attention as means through which significant energy reductions can be achieved . During the last decade, a number of investigations have been conducted on the design and modelling of different heat pump systems. This paper examines the performance of a solar assisted air source heat pump (ASHP) system for cold climate. The study compares the operation of a stand-alone ASHP against the solar assisted ASHP. The experimental measurements are used to test the performance of the ASHP system in different operating conditions. In addition, using TRNSYS (Transient Systems Simulation) software, simulation models were developed. The simulations using TRNSYS are compared to experimental data. Validation results for system modes of operation are included which demonstrate good conformity between model and experimental performance.

Peer-review under responsibility of Riga Technical University, Institute of Energy Systems and Environment.

Keywords: air source heat pump; unglazed transpired solar collector; COP; TRNSYS; simulation; model validation

1. Introduction

Various heat pump systems provide sustainable and efficient solutions to provide energy for space heating or cooling and domestic hot water in buildings [1]. There are millions of such systems installations worldwide and any improvement in heat pump systems, their operation and maintenance can save a considerable amount of energy, cost, and reduce global CO_2 emissions [2, 3]. Air source heat pumps (ASHPs) are widely applied as an economic

* Corresponding author: Tel.: +370 5 274 4718
E-mail address: karolis.janusevicius@vgtu.lt

Peer-review under responsibility of Riga Technical University, Institute of Energy Systems and Environment.
doi:10.1016/j.egypro.2016.09.039

form of heating [4]. However, one of the largest problems in ASHP systems is evaporator frosting, and the subsequent need for defrosting at low ambient temperatures and high humidity. Frost formation on the outdoor heat exchanger of an ASHP occurs when the surface temperature is both below the dew point of the moist air and the freezing point and periodic defrosting is necessary [5].

The frosting-defrosting process causes significant problems (reduced energy efficiency, increased pressure drop on air-side and heating shutdown) [6–9]. Different solutions to delay frosting and improve defrosting efficiency were proposed (system with integrated solid desiccant, reverse-cycle defrosting, electric heating defrosting, hot water spray, etc.) [3, 8–11]. Reverse cycle defrosting is currently the most widely used defrosting method [3, 11]. The energy used for reverse cycle defrosting comes from three sources: the input power to compressor, the input power to indoor air fan and the thermal energy from indoor air [11]. The energy consumption due to the defrost cycles should be considered in calculating the heat pump performance. However, the calculation methods proposed by the European standards ignore this effect [8, 12].

Many studies report on the performance of the ASHP system under frosting conditions [3–7, 10–13]. The energy efficiency of ASHP systems can be increased by not only optimizing the operational parameters of existing systems but also by integrating new elements into such system or looking for new technical solutions. Cabrol and Rowley [13] suggested a floor-embedded heating system coupled to a modern ASHP that could reduce running costs and CO2 emissions. Touchie and Pressnail [14] presented the operation of an ASHP in thermal buffer zone created by an enclosed balcony space. Such solution can improve the coefficient of performance (COP) in cold temperatures. Kamel and Fung [15] developed a TRNSYS model to integrate a photovoltaic/thermal collector in a roof and coupled it with ASHP. This suggestion enables a highly efficient heating system in winter conditions.

Despite the large number of studies on the performance and technical solutions of an ASHP system, defrosting causes the periodic interruption of outdoor heating and degradation in winter heating efficiency. Therefore, this study suggests the idea of solar assisted ASHP to prevent the heat pump from frosting. Unglazed transpired solar collector (UTSC) technology is integrated with ASHP. Although UTSC is a relatively new development in solar collector technology, it can serve as an energy saving measure in building engineering systems [16]. The aim of this work is to determine the performance benefits of operating an ASHP with UTSC. TRNSYS simulation software is used to model the operation of ASHP and integrated system of ASHP with UTSC. Simulated results are compared with experimental data gathered in the Laboratory of Building Energy and Microclimate systems (BEMS) in Vilnius Gediminas Technical University. The results from this study could be used to improve the operation process of the ASHP system.

Nomenclature

COP	coefficient of performance	$X_{measured}$	measured value
c_p	specific heat capacity of fluid, kJ/(kg·K)	$X_{simulated}$	simulated value
I	electrical current, A		
t	temperature, ºC	*Greek letters*	
t_{in}	fluid temperature at the inlet, ºC	Δ_{curr}	deviation at current time step
t_{out}	fluid temperature at the outlet, ºC	Δ_{max}	maximum deviation
U	voltage, V (230 V)	ρ	fluid density, kg/m^3
$\dot{V}$	volumetric flow rate, m^3/h	τ_{period}	time period, min
WRMSE	weighted root mean square error	$cos\ (\varphi)$	power factor (0.82)

2. Systems description

Analyzed systems are used in the BEMS Laboratory in Department of Building Energetics of Vilnius Gediminas Technical University. This laboratory (113 m^2) is equipped with a number of renewable energy technologies and equipment which use renewable energy. An air-to-water heat pump (HP) as well as UTSC are used for heating of laboratory [16]. Fig. 1 illustrates the systems used in experiments.

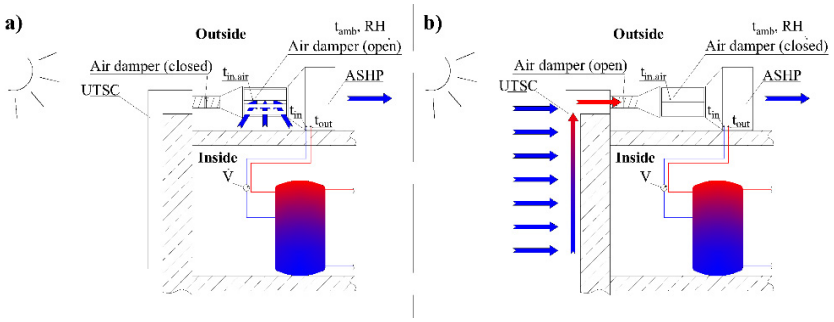

Fig. 1. Diagram of the analyzed systems: (a) operation of stand-alone ASHP (A case); (b) operation of ASHP combined with UTSC (B case).

The mixture of water and ethylene glycol of storage tank is heated by the air-to-water HP for both cases. When the ASHP operates alone in heating mode (case A) during the cold period, firstly it heats the storage tank. When ASHP operates with UTSC (case B), fresh air goes first through the UTSC where it is preheated.

UTSC technology. A perforated absorber plate is installed in a location where it is exposed to solar. UTSC intalled in the BEMS laboratory consists of three sections which differ by length and are equal to 3 m, 2 m and 1 m, respectively. Air goes from each section of UTSC to the main air duct. Its dimensions are 16.6 m in height and 6 m in width, the total area is 100 m^2. Airflow rate can be regulated with valves or stopped by closing the valves. The supply air temperature to the air handling unit can be changed by replacing the position of valves. The heat transfer of the transpired plate occurs at the front-of-plate, the holes and the back-of-plate.

ASHP technology. A variable-speed low temperature ASHP is selected. The ASHP was manufactured by Aermec (ANK020 HP), and has a rated COP of 2.57 (at condition A7/W55) in heating mode (heat capacity of 7.40 kW and electrical power of 2.88 kW).

3. Measurements and uncertainty

The main object of measurements is to calibrate simulation models (case A: operation of an ASHP and case B: operation of an ASHP with UTSC). The systems and their models were tested in the BEMS laboratory at local weather conditions. The selected periods presented are those when the outdoor air temperature ranged from –7 ºC to 7 ºC, a 1 min time interval was chosen for measurements.

For a value calculated from measurements of several individual values, the uncertainly of the resultant value is determined by applying the law of propagation of uncertainties of the individual values measured. It is assumed that the uncertainties are independent of one another and that each follows a normal Gaussian distribution. Thus, for instance, two randomly selected values might both have an uncertainty in the same direction [17].

The COP of the HP is evaluated as a ratio of heat capacity output and power input, expressed as:

$$COP = \frac{\dot{V} \cdot \rho \cdot c_p \cdot (t_{out} - t_{in})}{\sqrt{3} \cdot I \cdot U \cdot \cos(\varphi) \cdot 3.6} \quad (1)$$

The measured performance parameters (air temperature after heat exchanger, inlet and outlet water temperatures and electricity consumption) for both cases are plotted in Fig. 2. The results of uncertainty analysis for the physical parameters measured in this study are provided in Table 1. Uncertainty of measurements expresses quality of the experiment and at this case is important for calibration procedure.

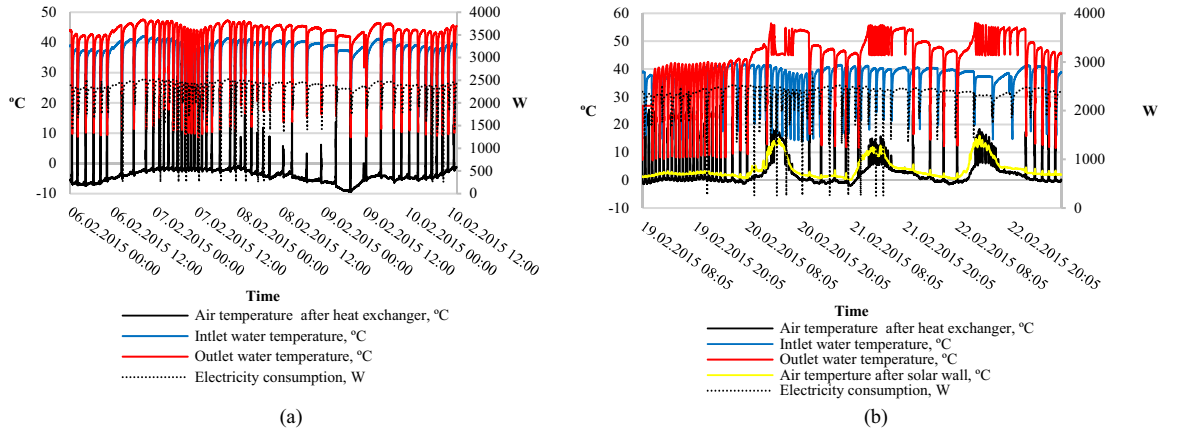

Fig. 2. Performance parameters of the ASHP (a) operation of the stand-alone ASHP; (b) operation of the ASHP combined with UTCS.

Where $\dot{V}_p$ is the permanent flow rate, the value 2.5 m^3/h is used. The permanent flow rate is the highest flow rate, at which the heat meter shall function continuously without the maximum permissible errors being exceeded. Using the uncertainty methodology described above, the maximum uncertainty of the COP for Case A is ±9.50 % and the minimum ±8.55 % when the ASHP operates under prescribed weather conditions.

Table 1. Measuring instruments and their specifications.

Measuring instrument	Measuring range	Accuracy of the primarily measured values
Temperature sensor PT500	–40 – 100 ºC	Class B: $\Delta t = \pm (0.3 + 0.005 \cdot (t))$ [18]
Flow meter	25 – 5000 l/h	Class 3: $\Delta t = \pm (3 + 0.05 \cdot \dot{V}_p / \dot{V})$, % [19]
Alternating current sensor	2 – 20 A	±4.5 % of full scale

Similar results are calculated for Case B (ASHP combined with UTSC), the maximum uncertainty for COP is ±9.86 % and the minimum uncertainty is ±8.53 %, respectively. According to the results, the uncertainty for both cases does not exceed 10 %. This indicates that experiments were carried out with reasonable uncertainty.

4. Models in TRNSYS

TRNSYS is a dynamic simulation tool developed over 30 years, with flexibility in modeling systems and buildings [20]. The model is executed at a 1 min time interval, as necessary to reflect control time constant. Mathematical models used to perform simulation in TRNSYS are described in the following subsections of the article.

4.1. ASHP model

For heat pump (HP) performance modeling Type 941, which represents operation based on performance map, is taken from manufacturer documentation [21]. Supplied data of heating capacity and consumed power for the given inlet air and water temperatures are used. The simulation model of ASHP operation was implemented in TRNSYS, as shown in Fig. 3, in which the equipment used and all their interconnections are depicted.

Typical HP models utilizing COP data from manufacturer documentations do not take into account an evaporator frost formation effects at negative outdoor temperatures. Advanced models like Type 401 [22] applies COP correction based on air temperature for whole operation temperature. There is a lack of real time impact models of frosting and defrosting period modeling due to the complex process of frost growing and the COP decrease due to lower heat transfer of the evaporator.

To reach a higher accuracy of the modeling and to make it possible to investigate the impact of different defrosting strategies on frosting duration, a model based on experimental data was used. The frosting model expresses time from one to the other defrosting period based on amount of condensation rates on evaporator and inlet temperature data. Such a data driven model was created by using MATLAB Curve fitting tool from measurement data. For this research we used this method to simulate the HP operation because the exact algorithm for this sequence of normal operation and defrosting was unknown due to commercial restrictions of HP manufacturer.

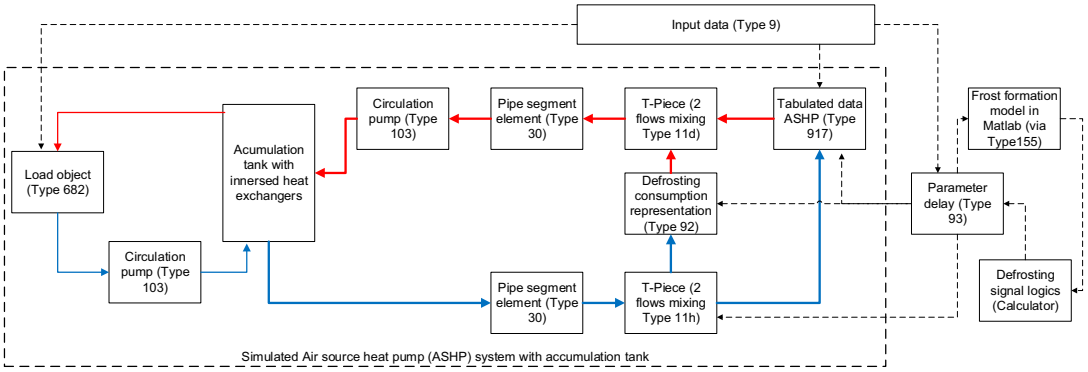

Fig. 3. ASHP model in TRNSYS environment.

In this case, an Airmeco HP is using reverse defrosting method, TRNSYS type 927 is switched off during defrosting period. According to measurements, the average defrost duration lasts approximately 11 minutes. During this period heat is taken out from the storage tank. The water flow is cooled at a rate equal to the energy amount needed to melt mass of frost accumulated on the evaporator – this action is simulated by using auxilary cooler (Type 92). Defrosting operation mode has high influence on the seasonal performance factor (SPF). Due to frosting and defrosting proceses influce to energy consumption this aspect should not be neglected from simulation model. It is important to take these effects in to account when building thermal comfort is assessed at short time periods.

Due to simplification reasons, COP degradation during frost formation on the evaporator is not taken into account. Only duration till total frosting is calculated and defrosting procedure with reverse cycle is simulated. Such configuration helps to evaluate short term effects which influence the degradation of the SPF of ASHPs connected to space or domestic hot water heating systems.

4.1. UTSC model

Type 561 models an unglazed solar collector that passes the air behind the plate which absorbs solar radiation. Moist air calculations are not included in this model. Thermal model of this type is based on the by Duffie and Beckman [23]. The type 561 from TRNSYS library operates with single inlet in the bottom of the plate and it does not reflect the actual situation of the analyzed UTSC installation at BEMS laboratory. Created simulation model combines multiple Types as UTSC segments. In order to reach a more realistic flow and surface temperature distribution, each segment gets its flow rate mixed from the bottom intake and part from ambient air sucked from air intake holes. This assumption creates the possibility to use the simulation model to predict collector surface temperature and helps to get a more realistic flow distribution along the collector height. Later this UTSC model is incorporated into the ASHP model and the new system is analyzed.

5. Models calibration

Calibration of model elements is an important step during preparation for complex simulation routines used for system design, accurate performance prediction and parametric studies. In this case, the following steps were taken:

- Select mathematical models suitable for particular elements for required time scale;
- Identify tuning parameters in mathematical models;
- Compare simulation and measurement data and express the differences with error function;
- Find parameters ensuring best model fitting measured data (outputs);

When experimental data is available as input and output, setting parameters of models could be done manually based on trial-and-error or by employing optimization tools. The goal of the calibration procedure is to find model parameters that ensure minimum possible value of error function. The mismatch is expressed using basic statistical expression – Weighted Root Mean Square Error (WRMSE) as a modified Root Mean Square Error (RMSE):

$$WRMSE = \sqrt{\frac{\sum_{period}\left(\left(\frac{\Delta_{\max}}{\Delta_{curr}}\right)\left(X_{measured} - X_{simulated}\right)^2\right)}{\sum_{period}\left(\frac{\Delta_{\max}}{\Delta_{curr}}\right)\cdot\tau_{period}}} \quad (2)$$

Calibration quality is assessed via mismatch function. This function expresses the cumulative difference between measured and simulated data points. In order to avoid error compensation in summation due to positive and negative differences, a comparison of single data point pair is squared before summation.

While measurement has uncertainty, this aspect should be taken into account during the calibration process. Assuming that points with greater uncertainty (higher measurement error) should have less influence when searching for parameters to fit curves, errors are counted as weight factors in the mismatch function. During the model calibration procedures, the parameters of TRNSYS types were adjusted to have better model fitting by minimizing the RMSE and WRMSE parameters. The lowest values of these statistical parameters ensure the closest match of simulated and measured data.

6. Results and discussion

Simulation model with technical parameters from documentation or initial parameters has a quite unacceptable discrepancy from measured data. Heat pump outlet temperature, UTSC outlet air temperature and heat pump COP as main indicators were chosen. To create the closest possible match, model parameters mentioned in Table 2 were adjusted. Separate component models and an overall system model was created within the TRNSYS Studio, then being parameterized (using table option in TRNEDIT) using variables and defining proper output files.

Table 2. Parameters adjusted during the model fitting.

Parameter	Submodel	Value
Air temperature limit for evaporator frosting	ASHP	3 °C
Total cumulated frost amount till defrosting	ASHP	200 [-]
Front loss coefficient	UTSC	67 W/m^{2}K
Back loss coefficient	UTSC	28 W/m^{2}K
Heat transfer rate	UTSC	82 W/m^{2}K

6.1. Measured and simulated values comparison

After adjustment of performance data used to simulate ASHP operation in TRNSYS type 927, a good conformity between simulated and measured data was reached using measured inlet water temperatures as model input (see Fig. 4a). The comparison between measured and simulated data of UTSC outlet air temperatures is shown in Fig. 4b.

Due to frosting effects, HP operation could not be simulated accurately when these effects are neglected as it is done in EN 15316-4-2 standard based methods. While manufacturers give performance data without frosting and there is no explained and standardized way to include frost formation and decrease the SPF due to defrosting periods, we used an empirical data driven frost formation model which helps to create better fit simulation model. This model reflects operation of the ASHP under frosting temperatures more accurately.

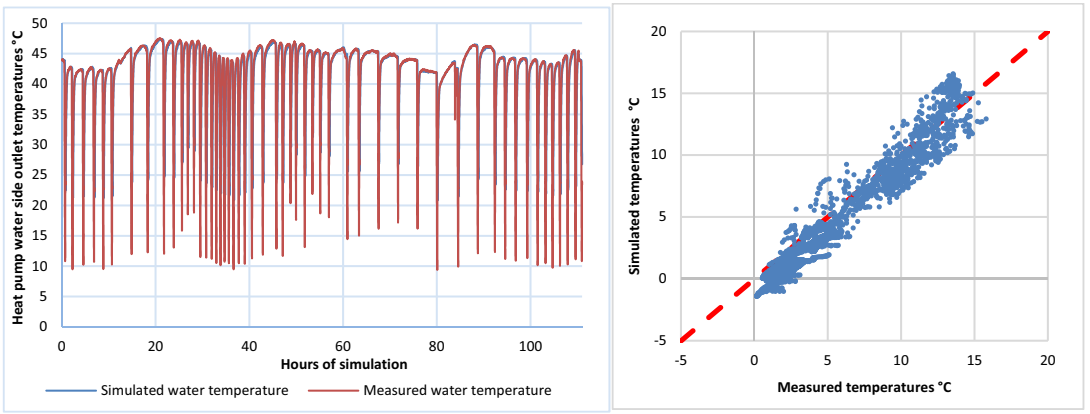

Fig. 4. Comparison of simulated and measured water temperatures after ASHP (a) and air temperature after UTSC (b).

In the ideal case when measured and simulated values match, all measurement points will appear on the dashed line (see Fig. 4 b). In the case when model is fitted with mismatch, some comparison points are below the line. This means that the model overestimates most of the values or predicts more pessimistic values than the real system has. In this case, the decrease of losses and increase of heat transfer in the UTSC model creates a higher mismatch. Due to this situation it was decided to accept the presented parameters as correct for model fitting.

6.2. Statistical evaluation

During the calibration procedure the statistical parameter WRMSE was examined and parameters ensuring the lowest error value were selected. By combining measurement uncertainty with model fitting, the overall prediction error could be expressed for absolute values. Uncertainty, fitting error and overall prediction values are shown in Table 3.

Table 3. Parameters adjusted during the model fitting.

Parameter	Measurement uncertainty	WRMSE	Overall prediction error
ASHP water outlet temperature	0.525 °C	0.56 °C	0.77 °C
ASHP COP	0.24 [-]	0.34 [-]	0.41 [-]
UTSC air outlet temperature	0.32 °C	1.34 °C	1.38 °C
ASHP with UTSC water outlet temperature	0.525 °C	0.91 °C	1.05 °C
ASHP with UTSC coefficient of performance	0.25 [-]	0.42 [-]	0.49 [-]

Thus a conclusion could be drawn that, when the ASHP is used with UTSC, the heat pump COP value could be predicted with an accuracy of 0.49. For these simulations the temperatures of the outlets from the HP and UTCS have absolute errors of 1.05 °C and 1.38 °C, respectively. If HP systems are designed to operate at a 5 degree temperature difference (which is typical), this model could predict energy consumption with an accuracy of 11 % for the periods when frosting appears on the evaporator. For periods without frost formation, ASHP performance could be predicted with greater accuracy due to the closer conditions of manufacturer declared data.

To reach higher accuracy of prediction models, they should be more complex and calibration periods should cover more operation conditions.

7. Conclusion

The performance characteristics of air source heat pump (ASHP) were experimentally investigated. The effects of the frost formation influence on operational performance as well as the combination with unglazed transpired solar collector to decrease frosting are discussed. The following conclusions can be made:

- Model is calibrated according to measurement data and the accuracy of simulation model predictions has a deviation of 11 % caused due to uncertainty in measurements and possible error due to model fitting;
- Typically used models neglect short term effects of frost formation and on air source heat pump evaporator. Examining possible improvement strategies for ASHP seasonal performance improvement, using of air preheating aspect has to be taken in to account. Authors suggest using the data driven frost formation model based on measurements, to capture short term effects;
- As a result simulation models were calibrated according to measured data by fitting TRNSYS component parameters and adding additional calculation routines to the simulation model used to predict solar assisted heat pump performance.

Acknowledgements

The authors would like to express their gratitude to the Building Energy and Microclimate Systems (BEMS) laboratory for the use of their TRNSYS and Matlab software and the possibility to use computational resources for model fitting.

References

[1] Januševičius K, Streckienė G. Solar Assisted Ground Source Heat Pump Performance in Nearly Zero Energy Building in Baltic Countries. Environmental and Climate Technologies 2013;11:48–56.
[2] Madani H. The Common and Costly Faults in Heat Pump Systems. Energy Procedia 2014;61:1803–6.
[3] Jang JY, Bae HH, Lee SJ, Ha MY. Continuous heating of an air-source heat pump during defrosting and improvement of energy efficiency. Applied Energy 2013;110:9–16.
[4] Guo X-M, Chen Y-G, Wang W-H, Chen C-Z. Experimental study on frost growth and dynamic performance of air source heat pump system. Applied Thermal Engineering 2008;28:2267–78.
[5] Kazjonovs J, Sipkevics A, Jakovics A, Dancigs A, Bajare D, Dancigs L. Performance Analysis of Air-to-Water Heat Pump in Latvian Climate Conditions. Environmental and Climate Technologies 2015;14(1);18–22.
[6] Zhang L, Fujinawa T, Saikawa M. A new method for preventing air-source heat pump water heaters from frosting. International Journal of Refrigeration 2012;35:1327–34.
[7] Chen Y, Guo X. Dynamic defrosting characteristics of air source heat pump and effects of outdoor air parameters on defrost cycle performance. Applied Thermal Engineering 2009;29:2701–2707.
[8] Schibuola L. Heat pump seasonal performance evaluation : a proposal for a European standard. Applied Thermal Engineering 2000;20:387–98.
[9] Jiang Y, Dong J, Qu M, Deng S, Yao Y. A novel defrosting control method based on the degree of refrigerant superheat for air source heat pumps. International Journal of Refrigeration 2013;36:2278–2288.
[10] Mengjie S, Xiangguo X, Shiming D, Ning M. An Experimental Study on Performance During Reverse Cycle Defrosting of an Air Source Heat Pump with a Horizontal Three-circuit Outdoor Coil. Energy Procedia 2014;61:92–5.
[11] Mengjie S, Dongmei P, Ning L, Shiming D. An experimental study on the negative effects of downwards flow of the melted frost over a multi-circuit outdoor coil in an air source heat pump during reverse cycle defrosting. Applied Energy 2015;138:598–604.
[12] Vocale P, Morini GL, Spiga M. Influence of Outdoor Air Conditions on the Air Source Heat Pumps Performance. Energy Procedia 2014;45:653–62.
[13] Cabrol L, Rowley P. Towards low carbon homes – A simulation analysis of building-integrated air-source heat pump systems. Energy and Buildings 2012;48:127–36.
[14] Touchie MF, Pressnail KD. Testing and simulation of a low-temperature air-source heat pump operating in a thermal buffer zone. Energy and Buildings 2014;75:149–59.
[15] Kamel RS, Fung AS. Modeling, simulation and feasibility analysis of residential BIPV/T+ASHP system in cold climate—Canada. Energy and Buildings 2014;82:758–70.
[16] Misevičiūtė V, Rudzinskas L. Simulation of ventilation system with unglazed solar collector and air heat pump. Presented at the 9th International Conference “Environmental Engineering”, Lithuania, Vilnius, 22–23 May; 2014.
[17] EN 12599:2000. Ventilation for building test procedures and measuring methods of handling over installed ventilation and air conditioning systems.
[18] Temperature Accuracy of Thermistors and RTDs. Available: http://www.bapihvac.com/content/uploads/Therm_vs_RTD.pdf
[19] EN 1434-1. Heat meters- Part 1: General requirements.
[20] Solar Energy Laboratory, Univ. of Wisconsin-Madison. TRNSYS 17 - a TRaNsient SYstem Simulation program. 2009
[21] Airmec Airmec Manual 2008.
[22] Afjej T, Wetter M. Compressor heat pump including frost and cycle losses. 1997.
[23] Duffie JA, William A. Beckman Solar Engineering of Thermal Processes. 4th Edition. Wiley; 2013.